Supporting Information

Influence of Dopant-Host Energy Level Offset on Thermoelectric Properties of Doped Organic Semiconductors

Bernhard Nell†, Katrin Ortstein†, Olga V. Boltalina‡, Koen Vandewal*†¶

†Dresden Integrated Center for Applied Physics and Photonic Materials, Technische Universität Dresden, 01062 Dresden, Germany

‡Department of Chemistry, Colorado State University, Fort Collins, CO 80523, USA

¶Institute for Materials Research, IMEC-IMOMEC, Hasselt University, 3590 Diepenbeek, Belgium

E-mail: bernhard.nell@iapp.de; koen.vandewal@uhasselt.be

Absorption spectra of $C_{60}F_{36}$ and $C_{60}F_{48}$ doped films

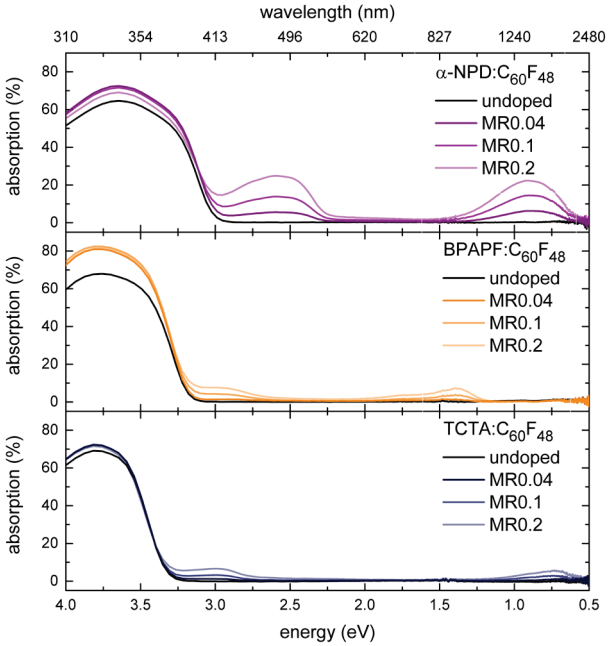

Figure S1|UV-VIS-NIR absorption of 100 nm α-NPD, BPAPF and TCTA doped with $C_{60}F_{48}$.

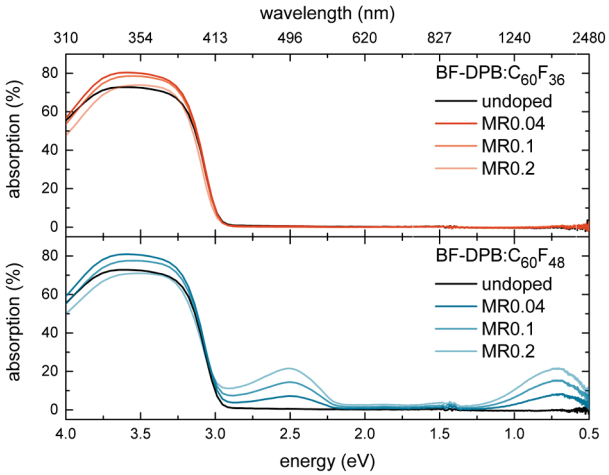

Figure S2| UV-VIS-NIR absorption of 100 nm BF-DPB doped with $C_{60}F_{36}$ and $C_{60}F_{48}$.

Absorbance of CN6-CP and $C_{60}F_{48}$-doped films

The estimation of the doping efficiency is performed on the absorbance A (Figures S3-S6) of doped films using Beer-Lambert-Law

$$\mathrm{A} = \log_{10}\left(\frac{I_0}{I}\right) = \varepsilon_\lambda \cdot c \cdot d$$

I_0……Intensity of incoming light

I……Intensity of transmitted light

ε_λ……molar extinction coefficient

c……molar concentration

d……film thickness

Table S1|material's properties

Film	**BF-DPB**	**α-NPD**	**BPAPF**	**TCTA**
Molar Mass [g/mol]	720.94	558.74	957.20	740.89
Density [g/cm³]	1.21	1.14	1.2	1.14

The molar extinction coefficient is calculated from the film thickness, and molar mass and film densities of the molecules (Table S1) in order to extract the concentration of ionized species. Doping efficiency of CN6-CP was estimated by comparing the integrated anion absorption peaks. That of $C_{60}F_{48}$ was calculated from the integrated molar absorbance of the NIR peaks of the $C_{60}F_{48}$-doped samples weighted by the ratio between the anion absorption and the NIR cation absorption of the CN6-CP doped films. Peak parameter of the CN6-CP anion can be found in table S2, NIR-cation peak parameter in tables S3-S6. $C_{60}F_{48}$ doped films were prepared at a host thickness of 100 nm. CN6-CP doped films at 40 nm for BF-DPB, α-NPD, BPAPF and 50 nm for TCTA.

Table S2|CN6-CP anion peak fit parameters

Film	**$\lambda_{max,1}$ [eV]**	**FWHM₁ [eV]**	**$\lambda_{max,2}$ [eV]**	**FWHM₂ [eV]**	**$\lambda_{max,3}$ [eV]**	**FWHM₃ [eV]**	**Area**
BF-DPB:CN6-CP MR 0.36	1.81	0.18	2.03	0.19	2.28	0.28	0.022
α-NPD:CN6-CP MR 0.36	1.81	0.16	2.04	0.24	2.31	0.30	0.025
BPAPF:CN6-CP MR 0.36	1.80	0.17	2.01	0.26	2.25	0.32	0.015
TCTA:CN6-CP MR 0.36	1.81	0.22	2.03	0.26	2.21	0.36	0.009

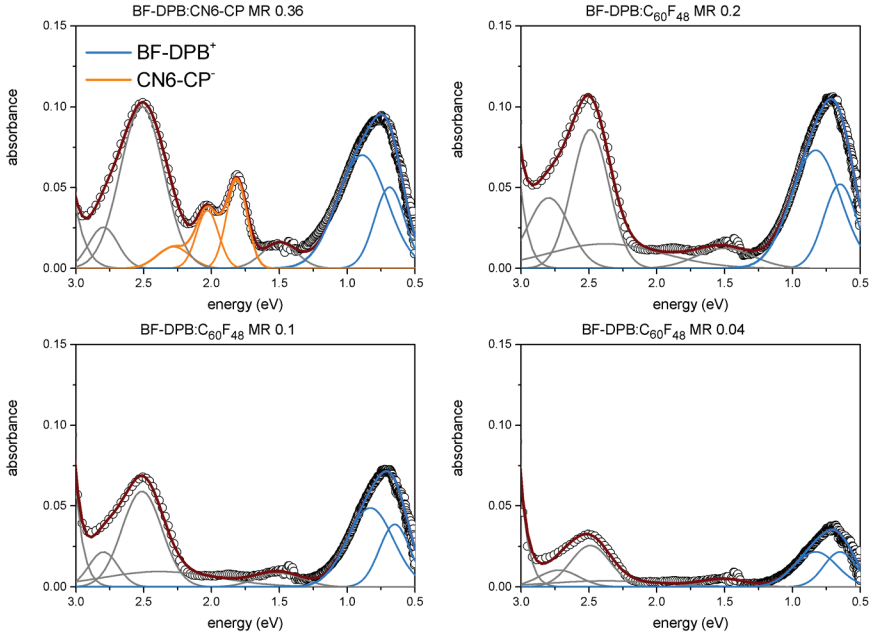

Figure S3|Absorbance of doped BF-DPB

Table S3|BF-DPB cation NIR peak fit parameters

Sample	**$\lambda_{max,1}$ [eV]**	**$FWHM_1$ [eV]**	**$\lambda_{max,2}$ [eV]**	**$FWHM_2$ [eV]**	**Area**
BF-DPB:CN6-CP MR 0.36	0.69	0.26	0.89	0.43	0.046
BF-DPB:$C_{60}F_{48}$ MR 0.04	0.65	0.28	0.83	0.37	0.015
BF-DPB:$C_{60}F_{48}$ MR 0.1	0.65	0.26	0.83	0.40	0.032
BF-DPB:$C_{60}F_{48}$ MR 0.2	0.65	0.28	0.83	0.43	0.049

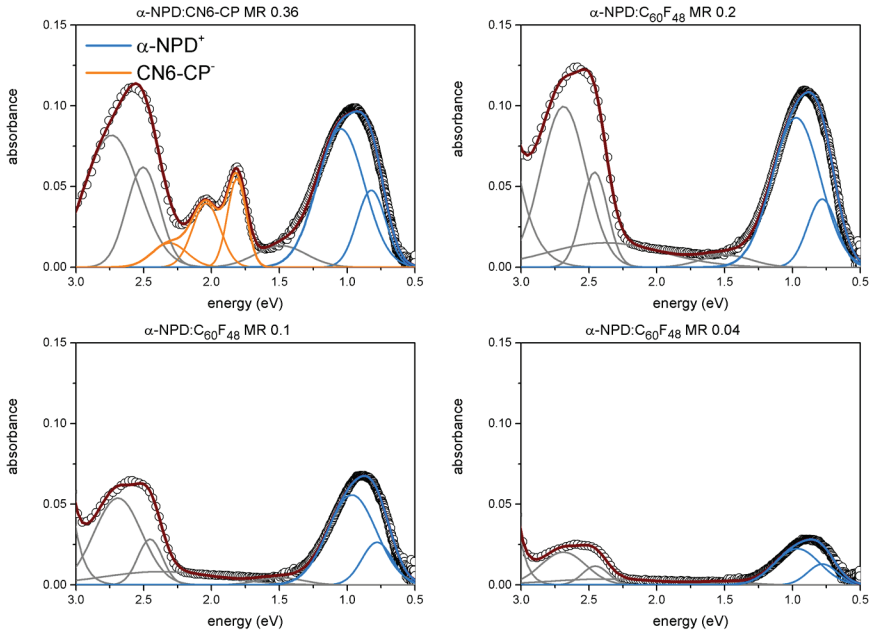

Figure S4|Absorbance of doped α-NPD

Table S4|α-NPD cation NIR peak fit parameters

Sample	**$\lambda_{max,1}$ [eV]**	**$FWHM_1$ [eV]**	**$\lambda_{max,2}$ [eV]**	**$FWHM_2$ [eV]**	**Area**
α-NPD:CN6-CP MR 0.36	0.82	0.25	1.05	0.41	0.050
α-NPD:$C_{60}F_{48}$ MR 0.04	0.78	0.25	0.96	0.39	0.013
α-NPD:$C_{60}F_{48}$ MR 0.1	0.78	0.26	0.96	0.42	0.032
α-NPD:$C_{60}F_{48}$ MR 0.2	0.78	0.25	0.97	0.42	0.053

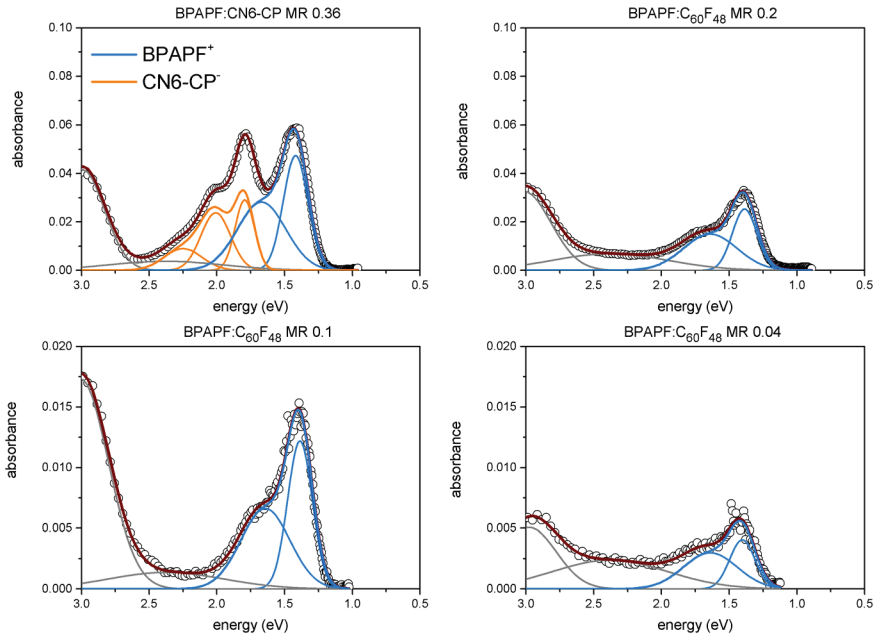

Figure S5|Absorbance of doped BPAPF

Table S5|BPAPF cation NIR peak fit parameters

Sample	**$\lambda_{max,1}$ [eV]**	**$FWHM_1$ [eV]**	**$\lambda_{max,2}$ [eV]**	**$FWHM_2$ [eV]**	**Area**
BPAPF:CN6-CP MR 0.36	1.42	0.21	1.67	0.42	0.0234
BPAPF:$C_{60}F_{48}$ MR 0.04	1.40	0.22	1.64	0.47	0.0024
BPAPF:$C_{60}F_{48}$ MR 0.1	1.39	0.21	1.64	0.43	0.0058
BPAPF:$C_{60}F_{48}$ MR 0.2	1.39	0.21	1.64	0.47	0.0132

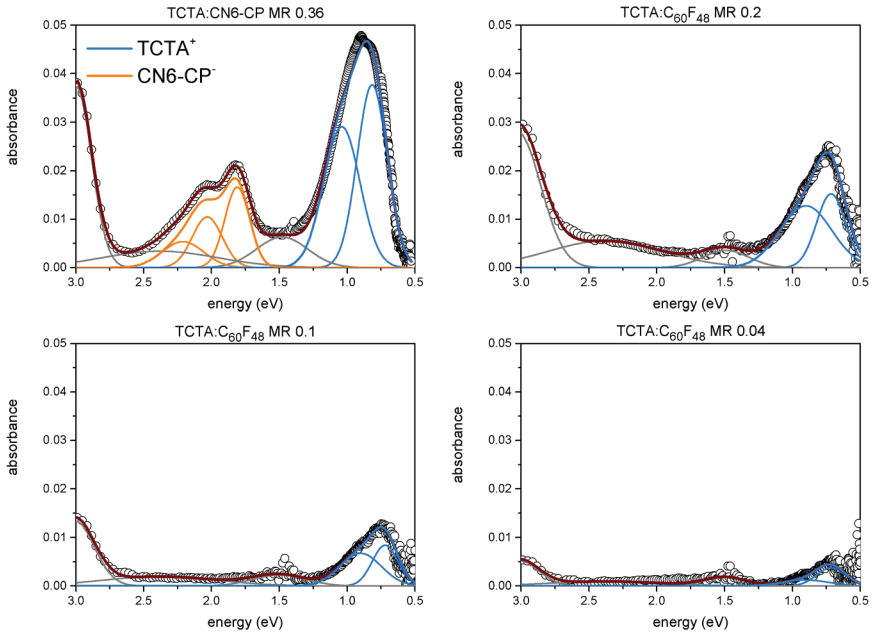

Figure S6|Absorbance of doped TCTA

Table S6|TCTA cation NIR peak fit parameters

Sample	**$\lambda_{max,1}$ [eV]**	**$FWHM_1$ [eV]**	**$\lambda_{max,2}$ [eV]**	**$FWHM_2$ [eV]**	**Area**
TCTA:CN6-CP MR 0.36	0.82	0.26	1.04	0.32	0.0203
TCTA:$C_{60}F_{48}$ MR 0.04	0.72	0.25	0.90	0.4	0.0015
TCTA:$C_{60}F_{48}$ MR 0.1	0.72	0.22	0.90	0.37	0.0045
TCTA:$C_{60}F_{48}$ MR 0.2	0.72	0.25	0.90	0.45	0.0102

Estimation of absolute doping efficiency

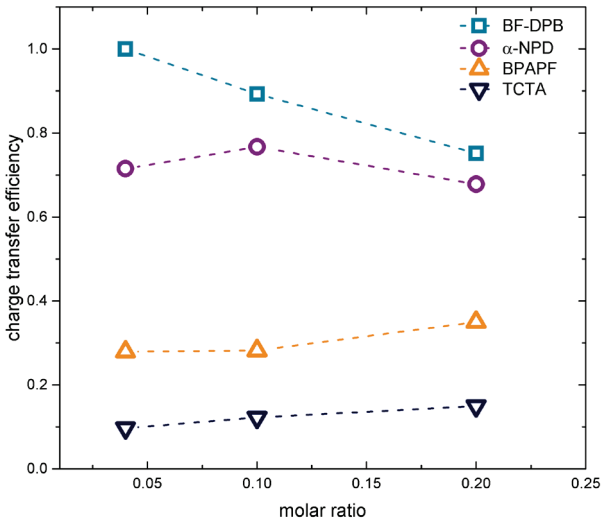

Figure S7| Charge transfer efficiency from UV-VIS-NIR measurements for $C_{60}F_{48}$ doped samples. Values are referenced to BF-DPB doped at MR 0.04.

Calculating charge transfer from charge neutrality equation

Charge transfer efficiency is calculated from numerically solving charge neutrality equation using Fermi-Dirac statistics. A Gaussian density of states is used for matrix and dopant states. The difference of the HOMO and LUMO maxima is related to electron affinity (EA) and ionization potential (IP) as D-A offset = IP-EA+4σ, with the width of the density of states σ. For the calculations in figure S9-S10 this corresponds to a dopant EA of 5.7 eV and 6.05 in Figure S11, using an intrinsic disorder of 0.1 eV. Procedure is describe in more detail elsewhere. [1,2]

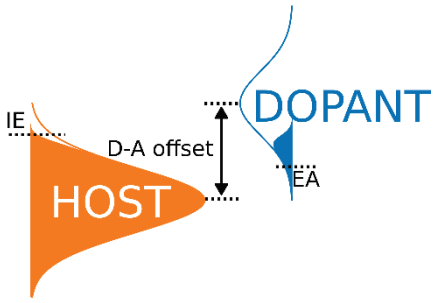

Figure S8|Charge transfer is calculated by solving charge neutrality equation for Gaussian density of states of matrix and dopant.

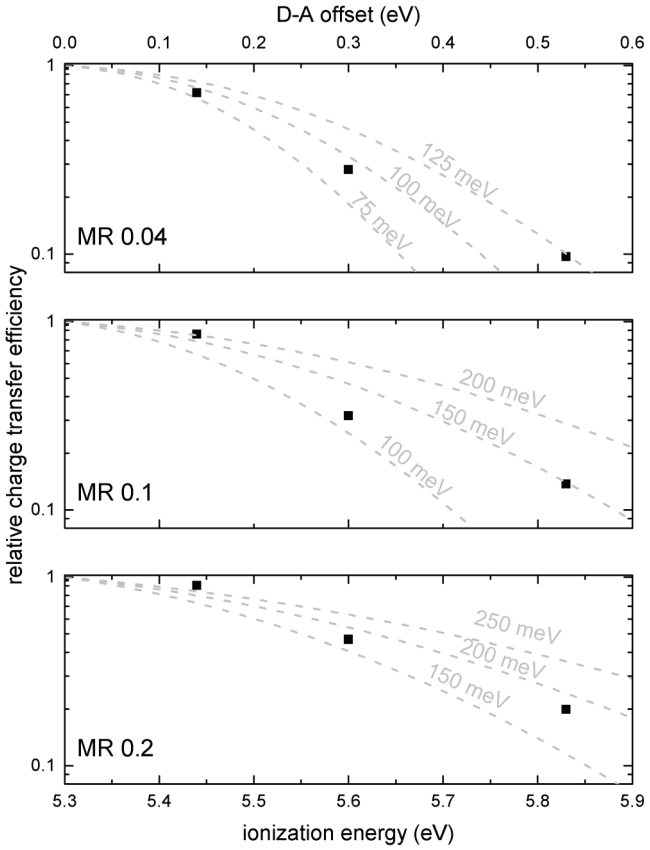

Figure S9|Relative doping efficiency for different doping concentrations. Symbols indicate values from absorption measurements using $C_{60}F_{48}$. Lines calculated by solving charge neutrality equation for Gaussian density of states for different DOS widths and D-A offsets.

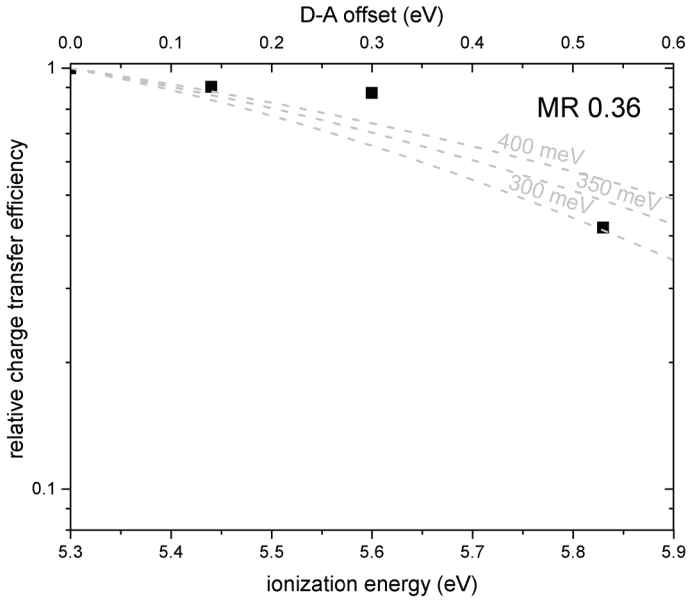

Figure S10|Relative doping efficiency for a molar doping ratio of 0.36 and the LUMO level of the dopant aligned with the HOMO of the host, compared to measurements on CN6-CP doped samples.

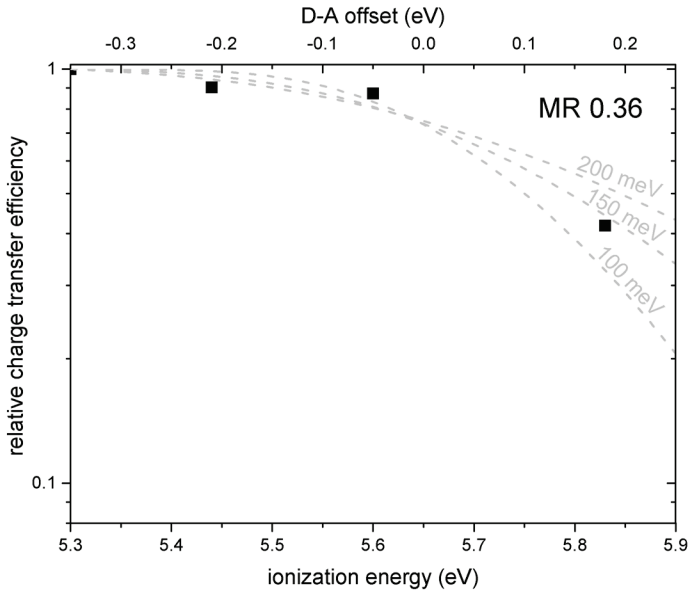

Figure S11|Relative doping efficiency for a molar doping ratio of 0.36 and the LUMO level of the dopant 0.35 eV lower than the HOMO of the host, compared to measurements on CN6-CP doped samples.

Ultra-violet photoelectron spectroscopy

Table S7|DOS widths determined by UPS

DOS width	**BF-DPB**	**α-NPD**	**BPAPF**	**TCTA**
σ_{UPS}[eV]	0.19	0.17	0.19	0.23

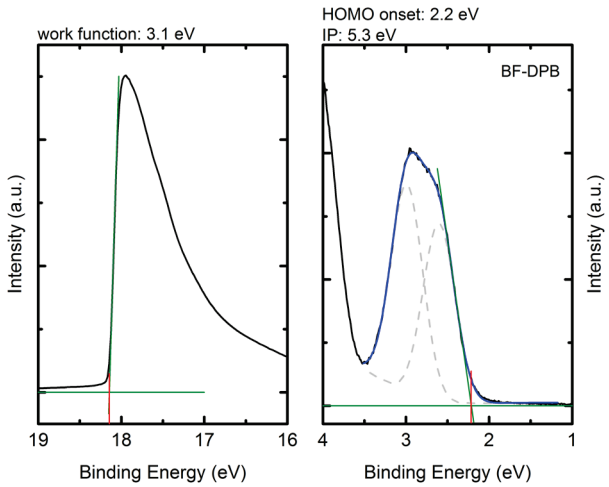

Figure S12|UPS spectrum of intrinsic BF-DPB on silver.

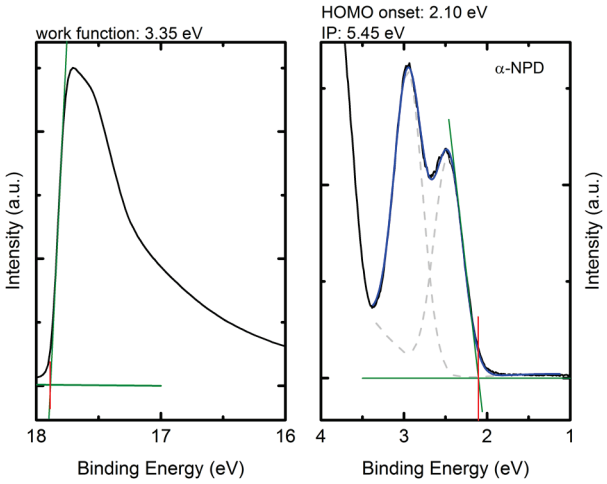

Figure S13| UPS spectrum of intrinsic α-NPD on silver.

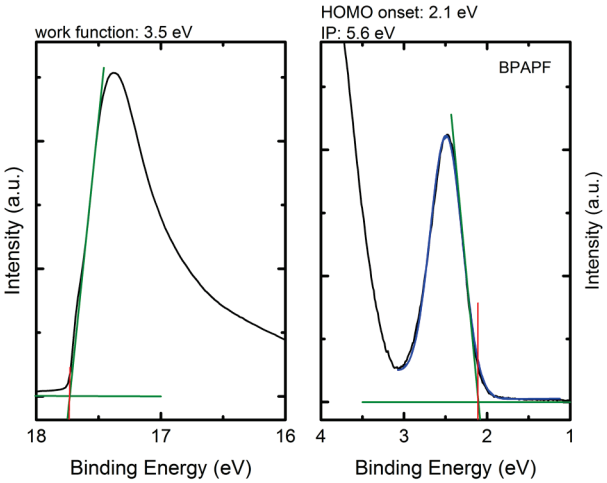

Figure S14| UPS spectrum of intrinsic BPAPF on silver.

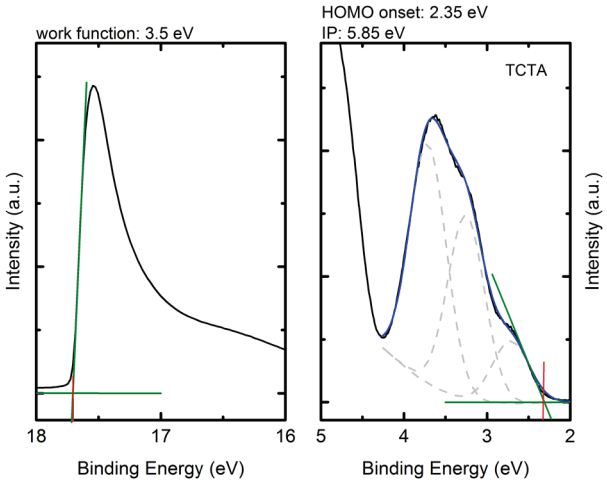

Figure S15| UPS spectrum of intrinsic TCTA on silver.

References

1. Tietze, M. L.; Pahner, P.: Schmidt, K.; Leo, K. & Lüssem, B. Doped Organic Semiconductors: Trap-Filling, Impurity Saturation, and Reserve Regimes. *Adv. Funct. Mater.* **2015,** *25*, 2701-2707.

2. Salzmann, I., Heimel, G., Oehzelt, M., Winkler, S. & Koch, N. Molecular Electrical Doping of Organic Semiconductors: Fundamental Mechanisms and Emerging Dopant Design Rules. *Acc. Chem. Res.* **2016,** *49*, 370-378.